

**NONLINEAR WHIRL RESPONSE OF A HIGH-SPEED SEAL TEST ROTOR  
WITH MARGINAL AND EXTENDED SQUEEZE-FILM DAMPERS**

**Margaret P. Proctor**

*NASA Glenn Research Center  
Margaret.P.Proctor@nasa.gov*

**Edgar J. Gunter**

*RODYN Vibration Analysis, Inc.  
DrGunter@aol.com*

**ABSTRACT**

Synchronous and nonsynchronous whirl response analysis of a double overhung, high-speed seal test rotor with ball bearings supported in 0.23- and 0.50-inch-long, uncentered squeeze-film oil dampers is presented. The design is similar to certain high-speed aircraft HP gas turbine rotors with squeeze-film oil dampers. Test performance with the original damper of length 0.23-inch was marginal, with nonsynchronous whirling at the overhung seal test disk and high amplitude synchronous response above 32,000 RPM near the drive spline section occurring. A system critical speed analysis of the drive system and the high-speed seal test rotor indicated that the first two critical speeds are associated with the seal test rotor. Nonlinear synchronous unbalance and time transient whirl studies were conducted on the seal test rotor with the original and extended damper lengths. With the original damper design, the nonlinear synchronous response showed that unbalance could cause damper lockup at 33,000 rpm. Alford cross-coupling forces were also included at the overhung seal test disk for the whirl analysis. Subsynchronous whirling at the seal test disk was observed in the nonlinear time transient analysis. With the extended damper length of 0.50 inch, the subsynchronous motion was eliminated and the rotor unbalance response was acceptable to 45,000 rpm with moderate rotor unbalance. However, the nonlinear analysis shows that with high rotor unbalances, damper lockup could also be obtained at 33,000 rpm, even with the extended squeeze-film dampers. Therefore, the test rotor must be reasonably balanced in order for the uncentered dampers to be effective.

**Keywords:** Nonlinear whirl response, squeeze-film dampers, damper lockup

**INTRODUCTION**

NASA has a high temperature, high speed seal rig to test seals over a range of conditions including conditions expected in advanced gas turbine engines. The double overhung rotor has an 8.5 inch seal test disk and is supported by rolling element bearings in squeeze film dampers to provide system damping. The maximum design speed of 43,140 rpm could not be achieved due to high vibrations at the seal test disk and at the spline connection to the drive shaft. There were indications of both sub- and super-harmonic whirl motion at the seal test disk and high synchronous response at the balance piston and drive spline. Experimental data indicated both a critical speed and whirling problem with the rig. Dynamic analysis indicated that enhancing the damper length would improve performance.

## 1. SEAL TEST ROTOR

### 1.1 Description of Rotor System and Instrumentation

The seal test rotor, shown in Figure 1, consists of a high temperature alloy shaft with two overhung disks. The test rotor is supported in two rolling element bearings. These bearings are in turn supported in squeeze film damper bearings.

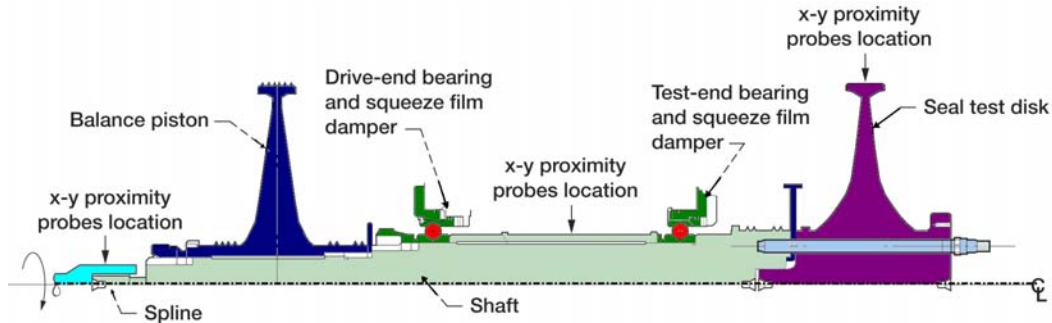


Figure 1 Seal Test Rotor Showing X-Y Proximity Probe Locations

The 8.5-inch, overhung seal test disk is piloted into the end of the shaft and clamped in place with six studs and retaining nuts. A test end insert is clamped between the seal test disk and the shaft and provides a rotor for a single knife-edge, which is part of an air buffer seal that prevents hot gases from reaching the oil-lubricated bearings. The balance piston is mounted on the opposite end of the shaft and is retained by a stainless steel lock washer and locknut. The split inner race angular contact ball bearings are mounted on the shaft between the two disks and separated by a bearing spacer. They are clamped in position by a shoulder on the shaft and a stainless steel lock washer and locknut. The bearings are mounted in oil squeeze-film dampers. The drive end of the shaft has an external spline. The drive system consists of a 60 hp air turbine and a torque meter connected to each other by a jack shaft with internal, straight splines at both ends. A similar jack shaft connects the torque meter to the seal test rotor. The alignment of the drive system to the seal test rotor is fixed by the housings for the jack shafts, torque meter and turbine, which pilot to each other and pilot to the seal test rig housing.

### 1.2 Instrumentation and Vibration

Proximity probes are used to observe the seal test rotor's dynamic performance. Eddy-current proximity probes at the spline and mid-span between the bearings are located at the 9 and 12 o'clock positions, when looking from the seal test disk towards the drive end, to view shaft orbits. For some tests, high-temperature capacitance proximity probes are installed at the 3, 6, 9, and 12 o'clock positions to view the seal test disk orbit and centrifugal growth. X-Y accelerometer pairs are mounted on the seal tester housing near the drive end bearings at the 9 and 12 o'clock positions and on the air turbine at the 12 and 3 o'clock positions. These measurements along with shaft speed are recorded on a digital tape recorder. Orbits are monitored on oscilloscopes and a spectrum analyzer is used to look at the amplitude and frequency content of the signals.

#### Test Rig X-Y Synchronous Accel Measurements

Fig. 3 represents the seal test rig synchronous X and Y accelerometer vs speed to 34,000 RPM. An apparent vertical system resonant mode is observed at 20,000 RPM. A much stronger resonance mode for the X accelerometer observed at 32,000 RPM. The difference between the

vertical and horizontal accel readings is due to the differences in bearing and support horizontal and vertical stiffness and damping values for the two planes. This asymmetry effect is often observed in uncentered dampers with moderate unbalances. Fig.4 shows the synchronous vertical turbine accel values as rotor speed increases. Above 32,000 RPM, there is observed a rapid increase in the turbine synchronous response measurement. There was also observed fractional frequency whirl motion in the turbine orbits at higher speeds. A further increase in the seal test rotor speed to its design speed of over 40,000 RPM could have resulted in rig damage.

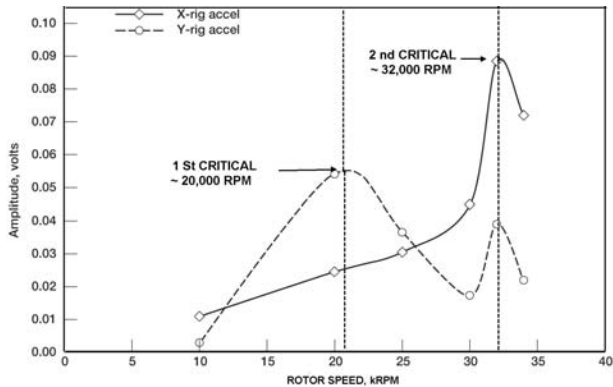


Fig. 3 X-Y Rig Synchronous Accel Vs Speed

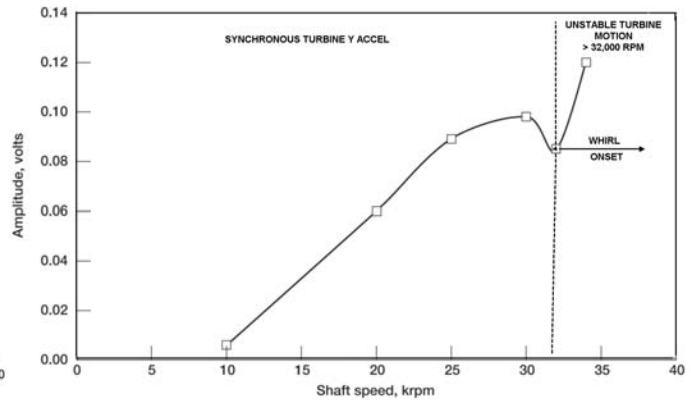


Fig 4 Turbine Y Synchronous Accel Vs Speed

### Seal Test Disk Orbits

Fig. 5 represents an orbit obtained from the seal disk. Note the occurrence of the double loop. Subharmonics of  $\frac{1}{2}$ ,  $\frac{1}{3}$  and superharmonics have been observed. This could be an indication of rubbing. Fig 6 represents a time exposure of the seal test disk motion. The orbital motion indicates impeller whirling. Above 32,000 RPM, the whirl motion increases.

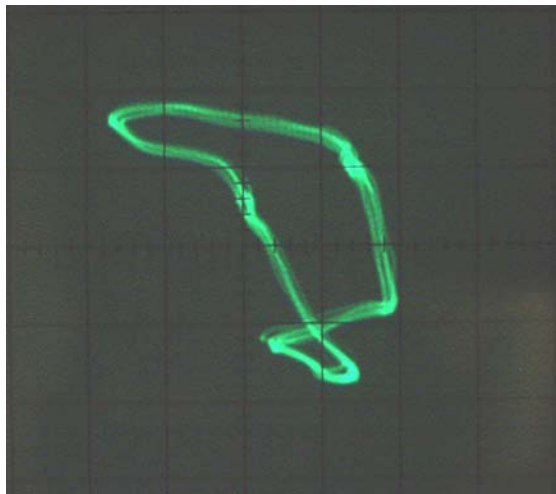


Fig. 5 Seal Test Disk Orbit With Double Loop

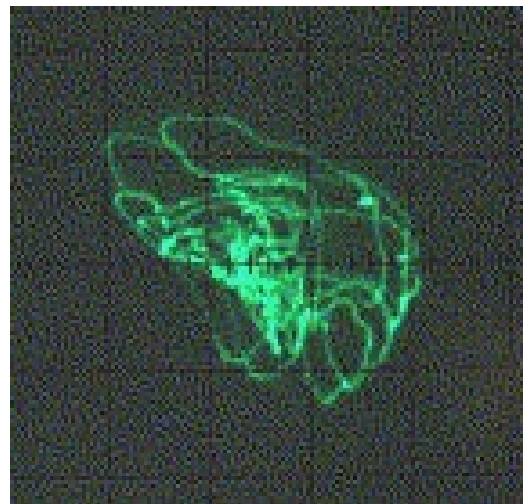


Fig. 6 Seal Test Disk Showing Nonsynchronous Whirling

## 2. CRITICAL SPEED ANALYSIS

### 2.1 Critical Speed Analysis of Test Rig

As a first step in the evaluation of the dynamical characteristics of the seal test rig, a model was generated of the entire test system including the drive turbine, torque tube and spline shafts. Since high vibrations are also encountered at the drive end spline connecting the seal test rotor, it

was important to determine if the drive system could be a contributing factor. Fig 7 represents the system first critical speed. With the nominal bearing values selected, it is seen the first system critical speed is a conical mode of the test rotor. The first critical speed in this model is 21,113 RPM. Note that Fig. 3 show a horizontal resonance around 20,000 RPM. This mode as show in Fig. 3 could be a conical whirling of the seals test rotor . With the conical motion, the bearing amplitudes are large and hence high damping should be provided in this mode.

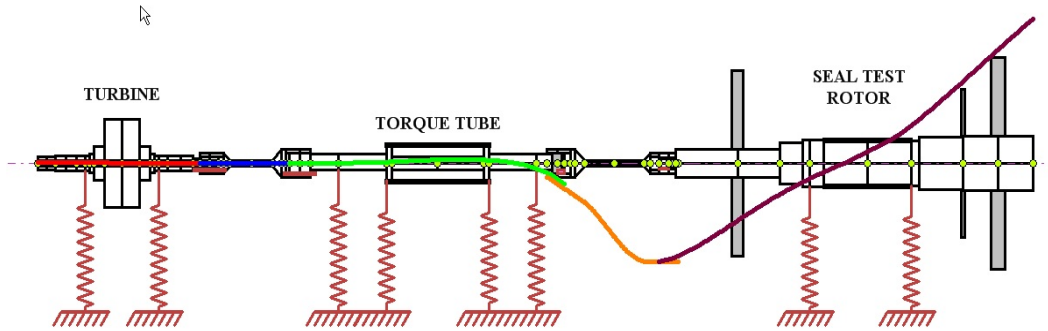


Fig. 7 Test Rig 1<sup>st</sup> Critical Speed at 21,113 RPM Showing Conical Seal Test Rotor Motion

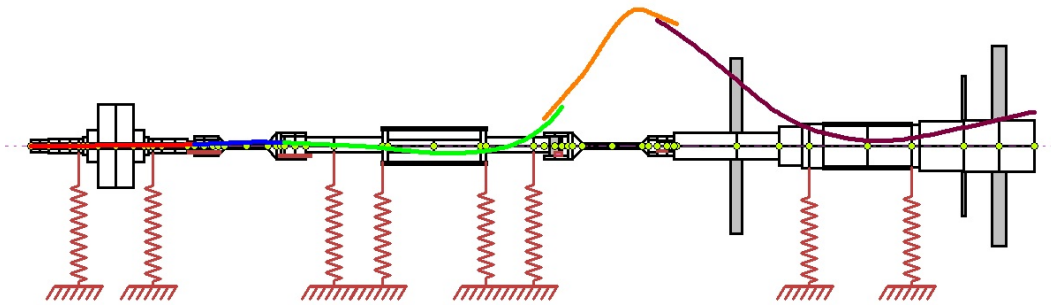


Fig. 8 Test Rig 2nd Critical Speed at 33,500 RPM RPM Showing High Drive Spline Motion- Balance Piston and Seal Impeller In Phase

Fig. 8 represents the system second critical speed mode at approximately 33,000 RPM. This high amplitude of motion at the drive spline could cause the spline to become disconnected. In the second mode, there is more strain energy in bending than in the 1<sup>st</sup> mode. The majority of the strain energy for the 1<sup>st</sup> mode is in the test rotor bearings. From an examination of the system strain and kinetic energies, it is noted that the first 2 system modes are related to the seal test rotor and the drive components may be ignored.

## 2.2 Critical Speed Analysis of Seal Test Rotor

### Seal Test Rotor Model

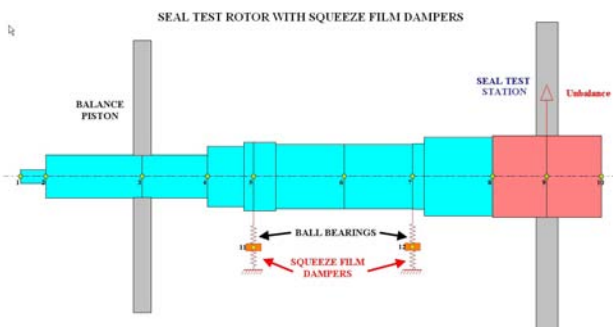


Fig. 9 Seal Test Rotor With Squeeze Film Dampers

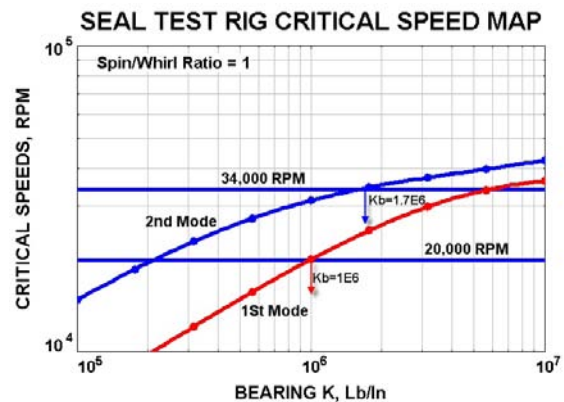


Fig 10 Critical Speed Map

**Seal Test Rotor Critical Speeds With Linear Bearings**

Fig. 9 represents a model of the seal test rotor. The rotor is supported in ball bearings. The rolling element bearings are in turn supported in uncentered squeeze film dampers. The analysis of the squeeze film damper is highly nonlinear. However, it is still of value to evaluate the rotor undamped critical speeds in order to determine the rotor mode shapes and the corresponding energy distribution for each mode.

Fig. 10 represents the critical speed map for the test rotor for the first two modes as a function of bearing stiffness. On the critical speed map are drawn the speed lines for 20,000 RPM and 34,000 RPM. With a nominal bearing stiffness value of 1e6 Lb/In, the 1<sup>st</sup> critical speed is predicted to be 20,000 RPM. This corresponds to the first frequency as seen in Fig. 3. As the speed increases, the bearing stiffness increases with loading. The 2<sup>nd</sup> critical speed is predicted to be 34,000 RPM for an assumed bearing stiffness of 1.7e6 Lb/In. as shown in Fig.10.

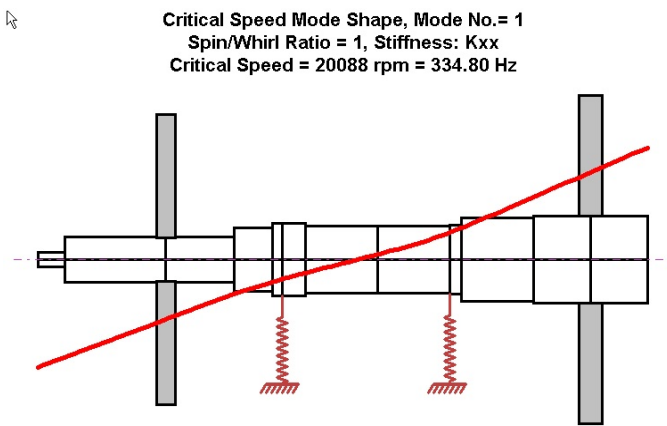


Fig 11 1<sup>st</sup> Mode at 20,000 RPM With Kb=1.0e6 Lb/In

Mode No.= 1, Critical Speed = 20088 rpm = 334.80 Hz  
Potential Energy Distribution (s/w=1)  
Overall: Shaft(S)= 19.14%, Bearing(Brg)= 80.86%

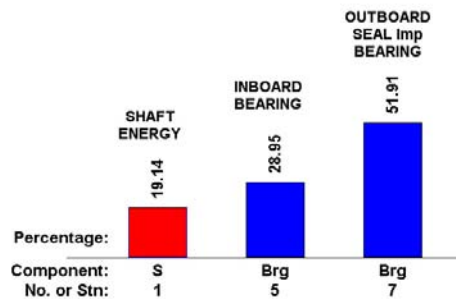


Fig. 12 1<sup>st</sup> Mode Potential Energy Distribution

Fig. 11 shows that the 1<sup>st</sup> mode is essentially a conical rigid body mode with the seal impeller and the balance piston out of phase. Fig. 12 represents the bearing and shaft relative potential or strain energy for this mode. Note that the outboard seal test end bearing contains over 50% of the system strain energy. Only 19% of the energy is in shaft bending. This also implies that 2 plane balancing will be sufficient to balance this mode. At higher shaft speeds, the outboard bearing will be the principal bearing required to control subsynchronous whirling.

Fig. 13 represents the second critical speed at 31,291 for an assumed bearing stiffness of 1.0e6 Lb/In stiffness. Fig. 14 shows the 2<sup>nd</sup> mode energy.

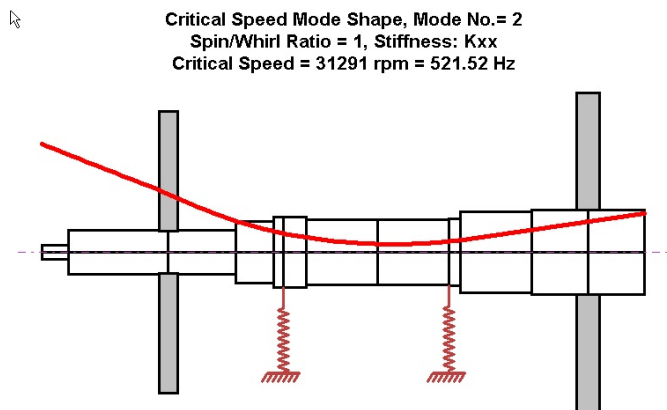


Fig. 13 2<sup>nd</sup> Mode At 31,291 RPM With Kb=1e6 Lb/In

Mode No.= 2, Critical Speed = 31291 rpm = 521.52 Hz  
Potential Energy Distribution (s/w=1)  
Overall: Shaft(S)= 59.60%, Bearing(Brg)= 40.40%

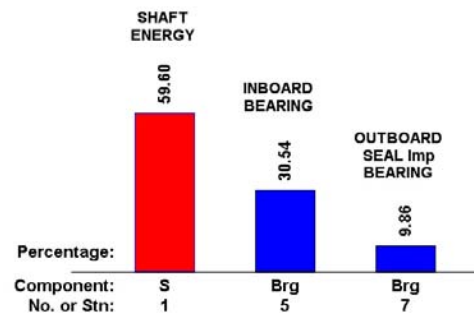


Fig. 14 2<sup>nd</sup> Mode Energy Distribution

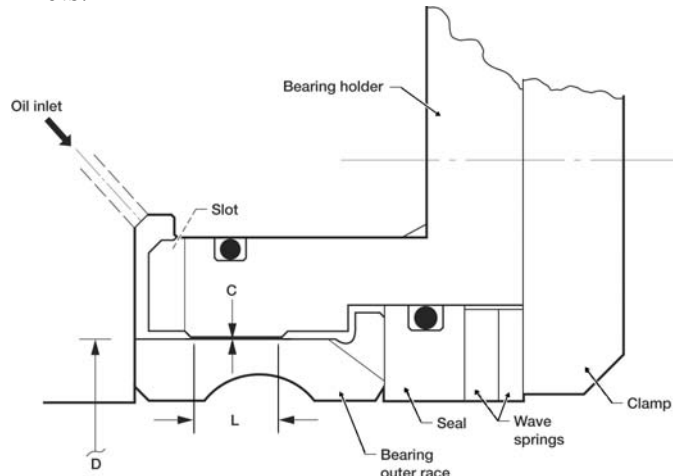
**Summary of Bearing Strain Energy For 1<sup>st</sup> 2<sup>nd</sup> Modes**

Fig. 12 shows that the outboard or test end bearing has a major influence on the first critical speed. From this can be implied that this is the principal bearing that must be modified to control subsynchronous whirl motion. Fig. 14 shows that the outboard bearing and damper have little control on the second critical speed. In order to control the second critical speed and high amplitude observed at the drive shaft location, the inboard bearing must be modified.

**3. DYNAMIC ANALYSIS WITH ORIGINAL SQUEEZE FILM DAMPER DESIGN**

**3.1 Squeeze-film Dampers**

The unbalance response of the seal test rig with the rolling element bearings mounted in squeeze film dampers is highly nonlinear in nature. The squeeze-film dampers are formed by the geometry of the bearing holder and the outer race of the bearing. The test end squeeze film damper, shown in Fig. 15 is formed at 2.90-inch diameter D, has a length L of 0.23 inch, and has a radial clearance C of 0.002 inch. MIL-23699 oil is supplied to the damper through 3 oil inlets.



**Fig. 15 Seal Impeller Damper Bearing**

The slot in the left end of the bearing holder provides a route for thermocouple wires that measure the bearing outer race temperature. There is no path for the oil to exit the test end squeeze film damper. The drive-end squeeze film damper has the same dimensions and is mounted in a similar fashion, except that oil can flow through it.

The damper is referred to as an uncentered squeeze film damper since it does not have a mechanical retaining spring. The damper design is similar to that encountered in various HP aircraft gas turbine rotors. Therefore, the damper

design and test results have significance towards design of damper bearings for various aircraft engine components.

**Squeeze Film Synchronous Stiffness and Damping Coefficients**

For the analysis of the synchronous unbalance of the test rotor, the bearing assembly is considered as a combination of the rolling element bearing in series with the uncentered squeeze film damper. The damper motion consists of precession but not rotation. Since the damper aspect ratio  $L/D < 1$ , the short bearing pi film version of Reynolds equation may be applied. For the case of unbalance response, a further assumption is made concerning the damper motion.. It is assumed that the motion is circular synchronous precession about the bearing center. This assumption is equivalent to the assumption that the rotating load exceeds the gravitational bearing loading. Under these assumptions, the nonlinear stiffness coefficient is given as follows:

$$K_d(\epsilon, \omega) = \frac{2 \mu R \epsilon \omega}{(1 - \epsilon^2)^2} \left( \frac{L}{C} \right)^3 \tag{1}$$

The damper radial stiffness  $K_d$  is a function of speed and eccentricity ratio. As the damper orbits outward to larger eccentricities, then the damper stiffness increases.

At eccentricity ratios above 0.9 then the radial damper stiffness becomes quite large. The effective stiffness of the bearing assembly then approaches the combined stiffness of the rolling element bearing and the bearing support system. This condition is referred to as damper lockup and is equivalent to dead band whirl in a rolling element bearing. High bearing forces occur under these circumstances. The corresponding damping coefficient is given by

$$C_d(\epsilon) = \frac{\pi \mu R}{2(1 - \epsilon^2)^{3/2}} \left(\frac{L}{C}\right)^3 \quad (2)$$

Eq. 2 shows the dramatic effect of an increase of the damper length L. A doubling of damper length results in an 8 fold increase in damping for the same eccentricity ratio.

### 3.2 Nonlinear Synchronous Unbalance Response With Original Damper Design

An unbalance response was computed with the original length dampers of 0.23 inches and a 2 mil radial clearance. Fig 16 represents the unbalance response with the nonlinear stiffness and damping coefficients as given in Eqs. 1 and 2.

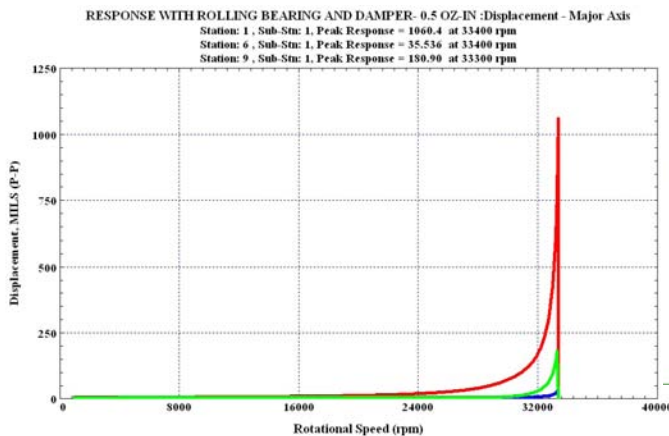


Fig. 16 Unbalance Response With Original Damper Design Showing Rotor Failure With 0.5 OZ-In

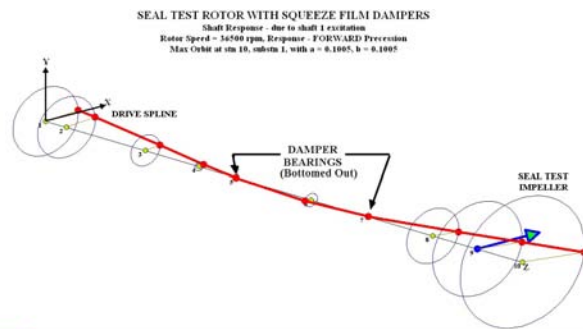


Fig. 17 Rotor Unbalance Mode Shape At 33,000 RPM Showing Damper Lockup

Fig. 16 shows that the synchronous unbalance response increases rapidly at speeds above 33,000 RPM. If the rotor speed were increased to the design speed of over 40,000 RPM, then test rotor damage could occur. Fig. 17 shows the 3 dimensional mode shape at 33,000 RPM. The unbalance is located on the seal test disk. The rotor rotating mode shape corresponds closely to the 2<sup>nd</sup> mode as shown in Fig. 13. In the unbalance response mode shape, note that the bearings are bottomed out. Since there is zero amplitude at the bearings, then there can be no contribution of damping from the bearings. Thus, when the squeeze film damper bearings bottom out or lockup, it is not possible to safely pass through the higher critical speed.

### 3.2 Time Transient Motion of Seal Test Rig With Original Damper Design

In the previous section on unbalance response, assumptions were made on the motion as to circular synchronous precession about the bearing origin. This shows useful information as to the high vibrations encountered at the drive spline In order to examine the possibility of nonsynchronous or whirl motion it is necessary to perform a time transient analysis.

Fig. 18 represents the time transient analysis options of the *DyRoBes* rotor dynamics program for the generalized rotor dynamic motion. In this case the Newmark-Beta method of integration was selected for the numerical procedure. Other options are 4<sup>th</sup> order Runge-Kutta and the Wilson Theta method. Selected in addition to unbalance is the gravitational loads as shown in Fig. 18. In

the time transient analysis, the damper forces are computed at each time step based on the damper instantaneous displacement and velocity values. No bearing coefficients are employed.

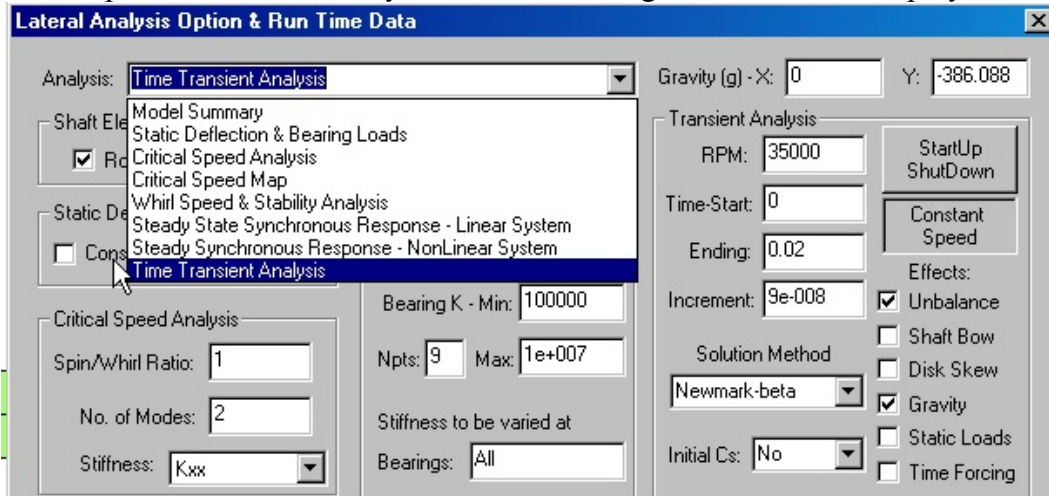


Fig. 18 Time Transient Analysis Options

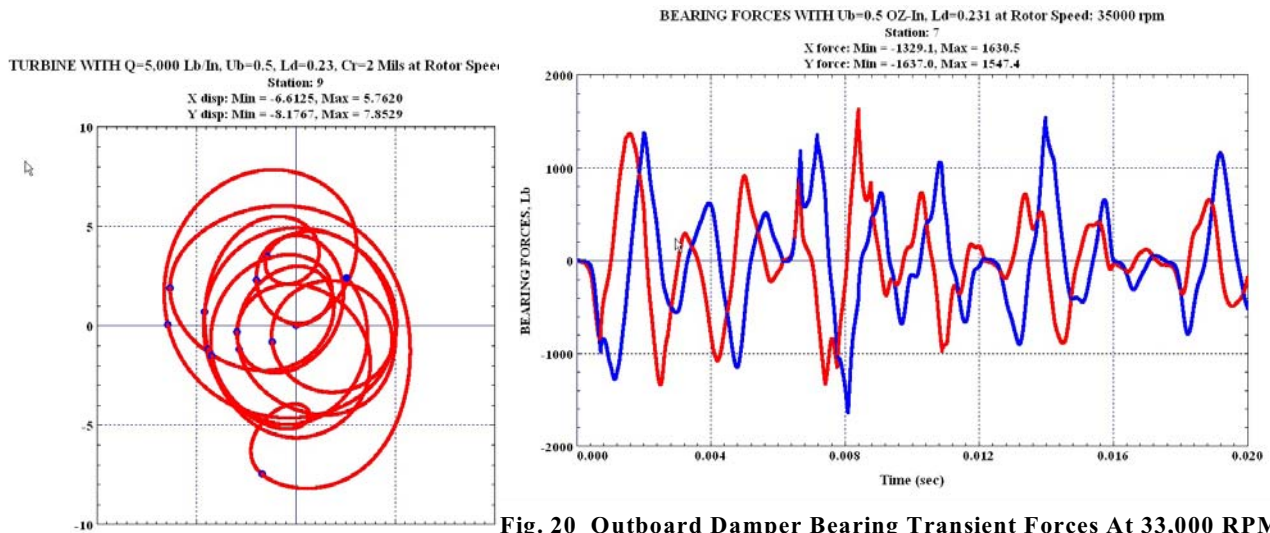


Fig. 20 Outboard Damper Bearing Transient Forces At 33,000 RPM

Fig. 19 Seal Impeller Orbit With Unbalance and Aero Cross Coupling Q=5,000 Lb/In at 33,000 RPM

Fig. 19 shows the transient motion of the seal test disk with suddenly applied unbalance and an assumed value of aerodynamic cross coupling coefficient of  $Q=5,000 \text{ Lb/In}$ . This Alford type effect is created by assuming a bearing station at the seal test disk and assigning  $K_{xy} = -K_{yx} = Q$ . The impeller orbit as shown in Fig. 19 indicates that the system is sensitive to small cross coupling forces that could be generated in typical seals. Fig. 19 indicates that the maximum orbit may exceed 8 mils. This could also lead to seal rubs which can generate super as well as subharmonic frequencies.

Fig. 20 shows the transient outboard bearing forces transmitted. These bearing loads are excessive and can result in diminished rolling element bearing life. The bearing loading is similar to the loads encountered with a rolling element bearing undergoing dead band whirl with a 2 mil clearance. It is apparent from the unbalance response plot of Fig. 16 and the whirl orbit as show

in Fig. 19 that the dampers are insufficient to provide adequate damping for control of seal test disk whirling or control of the high amplitude of vibration encountered at the drive spline at the 2<sup>nd</sup> critical speed.

#### 4. DYNAMIC ANALYSIS WITH ENHANCED SQUEEZE FILM DAMPERS

##### 4.1 Nonlinear Synchronous Unbalance Response With Enhanced Damper Design

It is apparent from the unbalance and whirl analysis of Section 3 that the squeeze film damping is inadequate. An analysis was performed with enhanced dampers with the damper length increased from 0.23 to 0.5 inches. Fig. 21 represents the unbalance response with the enhanced dampers and two planes of unbalance of 0.1 OZ-In at 90° relative phase. With improved damping and the reduced level of unbalance, the response is smooth to 50,000 RPM. Fig 22 represents the synchronous mode shape at 45,000 RPM. The rotor has little shaft bending.

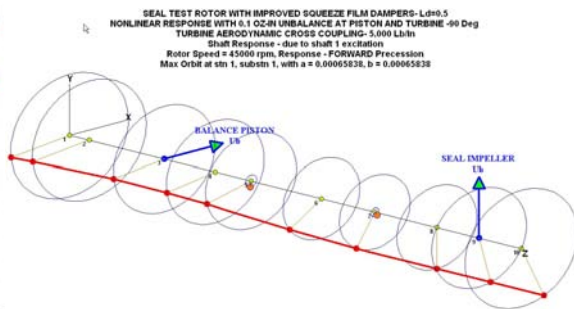
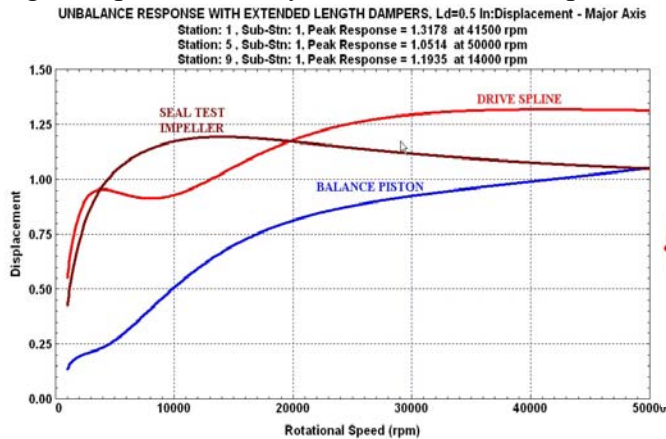


Fig. 22 Shaft Mode Shape at 45,000 RPM

Fig. 21 Unbalance Response With Enhanced Dampers With Unbalance=0.1 OZ-In @90 at Impeller And Balance Piston

##### 4.2 Time Transient Motion of Seal Test Rig With Enhanced Damper Design

##### Transient Motion At 35,000 RPM With 2 Planes Ub=0.1 And Aero Cross Coupling Q

Fig. 23 shows the transient response at 35,000 RPM. Note the conical shaft motion with active damper motion. Fig. 24 represents the outboard bearing forces transmitted. The initial 1<sup>st</sup> forward conical mode rapidly damps out leaving only the synchronous unbalance response. There is no indication of self excited whirl motion present in the transient data.

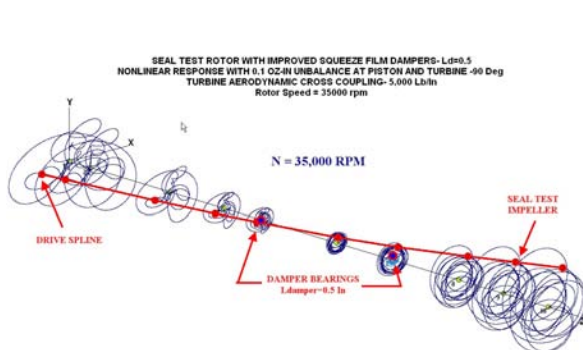


Fig. 23 Transient Rotor Motion at 35,000 RPM With Enhanced Squeeze Film Dampers, Ub=0.1

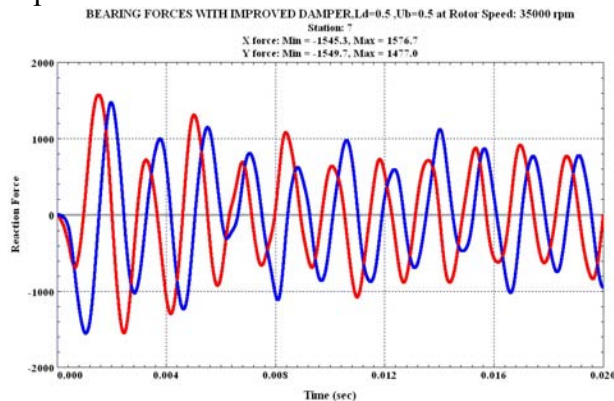


Fig. 24 Outboard Bearing Forces Transmitted

##### Transient Response At 45,000 RPM

Fig. 25 represents the transient motion at 45,000 RPM. The motion is stable limit cycle whirl.

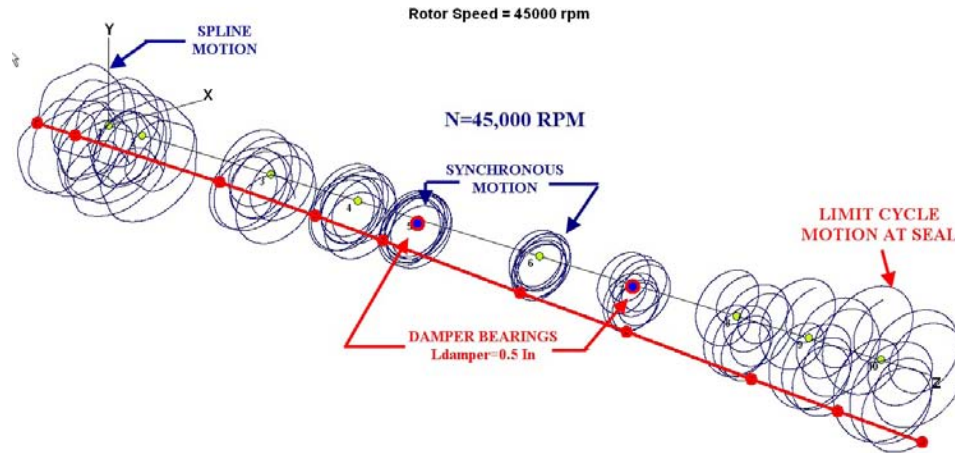


Fig. 25 Transient Motion At 45,000 RPM Showing Stable Limit Cycle Whirl Motion

### 4.3 Synchronous Response With High 2 Plane Unbalance, $U_b=0.5$ OZ-In

Fig. 25 represents the nonlinear unbalance response if the two planes of unbalance are increased from 0.1 to 0.5 OZ-In.

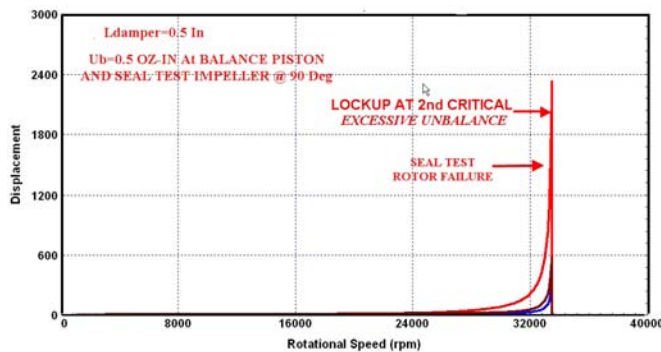


Fig. 26 Synchronous Response With High Unbalance

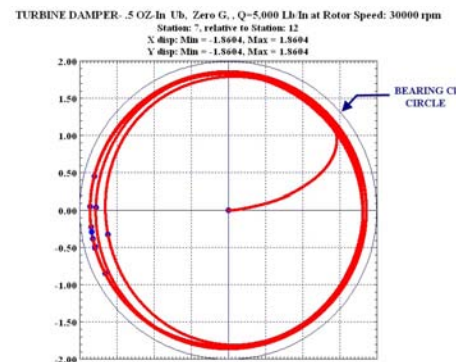


Fig. 27 Relative Damper Motion At 30,000 RPM Showing High Eccentricity

## 5. DISCUSSION AND CONCLUSIONS

In the design of high speed rotors mounted in rolling element bearings, it is necessary to provide some form of damped flexible support in order to pass through the critical speeds without bearing distress. In addition to the critical speed problem, damping at the bearings or support is also required to prevent self excited whirl motion caused by internal friction or Alford type of forces acting at impellers and balance pistons. A common type of damper employed with rolling element bearings is the squeeze film damper bearing. This bearing-damper configuration is very common in aircraft gas turbine engines. The damper may or may not have a centering spring. The centering spring is needed on heavily loaded rotors to support the gravitational loads. In the case of the seal test rig, the centering spring design was not used. The uncentered design used is similar to the design used in many aircraft LP and HP gas turbine rotors.

The design and analysis of this type of bearing is complicated by the nonlinear nature of the squeeze film damping characteristics. When the bearing is centered in the damper, the film stiffness is zero. As the bearing housing precesses in the damper clearance, the damper radial squeeze film stiffness increases rapidly. If the orbital motion in the damper exceeds 70% of the clearance, then damper lockup may occur. Even a well designed damper may experience damper lockup with excessive unbalance. Computer simulation is required for proper design.